GLS Approximations for Quasi-Newtonian Fluid Flows

Flávia Zinani[1] and Sérgio Frey[2]

[1] Universidade do Vale do Rio dos Sinos, Porto Alegre, Brazil.
2 Federal University of Rio Grande do Sul, Porto Alegre, Brazil.

ABSTRACT

This article uses a multi-field Galerkin least-squares (GLS) method for approximating flow-type sensitive fluid flows. A quasi-Newtonian model, based on a kinematic parameter of flow classification and shear and extensional viscosities, is employed to represent the fluid behaviour from pure shear up to pure extension. Mild Weissenberg flows of quasi-Newtonian fluids – using Carreau viscosities with power-law indexes varying from 0.2 to 2.5 – are carried out through a four-to-one planar contraction.

INTRODUCTION

This article addresses a class of flow-type sensitive fluids called quasi-Newtonian models. Their major features are the viscosity function dependent of the flow type and the extra-stress tensor described by the generalized Newtonian model (GNL). The quasi-Newtonian fluid flows herein considered are approximated by a multi-field (GLS) method in terms of strain rate, pressure and velocity. Due to the addition of residual-based least-squares terms of the flow governing equations, the GLS method allows the use of simple combinations of finite element interpolations and remains stable even in flows subjected to high geometric and material non-linearity. The flow domain is 4:1 sudden planar contraction and the triple ($\mathbf{D}$-p-$\mathbf{u}$) is approximated by a combination of bi-linear Lagrangian interpolation for pressure, and bi-quadratic ones for strain rate and velocity. The bi-quadratic interpolation for the tensor $\mathbf{D}$ assures an accurate representation of the flow classifier, which depends on the first derivatives of $\mathbf{D}$. For a relevant range of Weissenberg number for such a problem (Wi from 0 to 0.6), three flow-type sensitive fluids are investigated: (i) a shear-thinning fluid; (ii) an extension-thickening fluid; (iii) and a shear-thinning and extension-thickening fluid. For all fluids, the distribution of the flow classifier is evaluated, capturing both extensional flow regions in the contraction vicinity and pure shear flows far away from the contraction.

THE QUASI-NEWTONIAN MODEL

From the usual momentum and mass balance equations for a incompressible fluids, coupled with the GNL constitutive equation, a ($\mathbf{d}$-p-$\mathbf{u}$) boundary value problem, for steady flows of purely viscous fluids, may be stated as:

$$
\begin{aligned}
&\rho[\nabla\mathbf{u}]\mathbf{u}-2\eta(R_r,II_{\mathbf{D}})\operatorname{div}\mathbf{d} \\
&-2\nabla(\eta(R_r,II_{\mathbf{D}}))\cdot\mathbf{d}+\nabla p=\rho\mathbf{g} && \text{in } \Omega \\
&\mathbf{d}-\mathbf{D}(\mathbf{u})=0 && \text{in } \Omega \\
&\operatorname{div}\mathbf{u}=0 && \text{in } \Omega \\
&\mathbf{u}=\mathbf{u}_g && \text{on } \Gamma_g \\
&[-p\mathbf{1}+2\eta(R_r,II_{\mathbf{D}})\mathbf{d}]\mathbf{n}=\mathbf{t}_h && \text{on } \Gamma_h
\end{aligned}
\tag{1}
$$

where $\mathbf{u}$ is the fluid velocity, p the pressure, ρ the density, $\mathbf{d}$ and $\mathbf{D}(\mathbf{u})$ are alternative

notations for the strain-rate tensor, $\mathbf{1}$ the unity tensor, $\mathbf{g}$ the gravitational acceleration, $\mathbf{n}$ the outward unity vector, $\mathbf{t}_h$ the stress vector and $\mathbf{T}$ is stress tensor , $\mathbf{T}=\boldsymbol{\tau}-p\mathbf{1}$.

The quasi-Newtonian viscosity function considered herein, $\eta(R_r, II_{\mathbf{D}})$, is given by a weighted mean between the shear viscosity η_s and the extensional viscosity η_x, both of them independently constructed according the Carreau equation,

$$\eta = \eta_s^{f(R_r)} \eta_x^{(1-f(R_r))}$$

$$\eta_s = \eta_{\infty_s} + (\eta_0 - \eta_{\infty_s})(1 + (\lambda_s \dot{y})^2)^{(n_s-1)/2} \qquad (2)$$

$$\eta_x = \eta_{\infty_x} + (\eta_0 - \eta_{\infty_x})(1 + (\lambda_x \dot{y})^2)^{(n_x-1)/2}$$

where the function $f(R_r)$ in Eq. (2) is the one proposed by Ryssel and Brunn[1],

$$f(R_r) = \frac{3\sin^4(R_r \pi/2)}{1 + 2\sin^4(R_r \pi/2)}, \; if \; 0 < R_r < 1 \qquad (3)$$
$$f(R_r) = 1 \qquad\qquad\quad , \; if \; (R_r > 1),$$

and R_r is a flow classifier based on the classifier R_R proposed by Thompson and Souza Mendes[2],

$$R_r = \frac{2R_R}{1 + R_R} \qquad (4)$$

and $\dot{y}$ and is the magnitude of tensor $\mathbf{D},$.

NUMERICAL METHOD

From the usual definitions of finite element subspaces for incompressible fluid flows (Behr et al.[3]), a three-field GLS formulation can be written as: given $\rho\mathbf{g}$ and $\boldsymbol{u}_g$, find the triple $(\mathbf{d}$-p-$\mathbf{u})$ such that:

$$\int_\Omega \mathbf{d}^h \cdot \mathbf{S}^h d\Omega - \int_\Omega \mathbf{D}(\mathbf{u}^h) \cdot \mathbf{S}^h d\Omega - \int_\Omega p^h \operatorname{div} \mathbf{v}^h d\Omega$$
$$+ \int_\Omega \rho[\nabla \mathbf{u}^h]\mathbf{u}^h \cdot \mathbf{v}^h d\Omega + \delta \int_\Omega \operatorname{div} \mathbf{u}^h \operatorname{div} \mathbf{v}^h d\Omega$$
$$+ \int_\Omega \operatorname{div} \mathbf{u}^h q^h d\Omega + \int_\Omega 2\eta(R_r, II_{\mathbf{D}})\mathbf{d}^h \cdot \mathbf{D}(\mathbf{v}^h) d\Omega$$
$$+ \sum_{K \in \Omega^h} \int_{\Omega_K} (\rho[\nabla \mathbf{u}^h]\mathbf{u}^h + \nabla p^h - 2\eta(R_r, II_{\mathbf{D}}) \operatorname{div} \mathbf{d}^h +$$
$$-2[\mathbf{d}^h]\nabla(\eta(R_r, II_{\mathbf{D}}))\cdot$$
$$\cdot \alpha(\operatorname{Re}_K)(\rho[\nabla \mathbf{v}^h]\mathbf{u}^h - \nabla q^h - 2\eta(R_r, II_{\mathbf{D}}) \operatorname{div} \mathbf{S}^h +$$
$$-2[\mathbf{S}^h]\nabla(\eta(R_r, II_{\mathbf{D}}))d\Omega_K$$
$$+ \beta \sum_{K \in \Omega^h} \int_{\Omega_K} 2\eta(\dot{y})(\mathbf{d}^h - \mathbf{D}(\mathbf{u}^h)) \cdot (\mathbf{S}^h - \mathbf{D}(\mathbf{v}^h))d\Omega_K$$
$$= \int_\Omega \rho\mathbf{g} \cdot \mathbf{v}^h d\Omega + \int_{\Gamma_h} \mathbf{t} \cdot \mathbf{v}^h d\Gamma$$
$$+ \sum_{K \in \Omega^h} \int_{\Omega_K} \rho\mathbf{g} \cdot \alpha(\operatorname{Re}_K)(\rho[\nabla \mathbf{v}^h]\mathbf{u}^h - \nabla q^h +$$
$$-2\eta(R_r, II_{\mathbf{D}}) \operatorname{div} \mathbf{S}^h - 2[\mathbf{d}^h]\nabla(\eta(R_r, II_{\mathbf{D}}))d\Omega_K$$
$$(5)$$

with the stability parameters δ, α, and β, associated to continuity, motion and quasi-Newton equations, respectively, being given by Franca and Frey[4] and Behr et al.[3].

RESULTS AND DISCUSSION

The geometry considered is a sudden 4:1 planar contraction, as shown in Fig. 1. For all computations, a combination of bi-quadratic/bi-linear/bi-quadratic finite elements (Q2/Q1/Q2) is used for the triple strain rate, pressure and velocity, respectively. After a mesh independence test, a mesh of 4,368 elements is chosen.
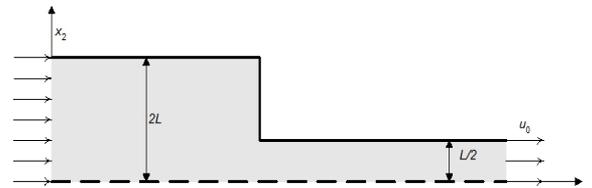

Figure 1. The problem statement.

The characteristic strain rate $\dot{y}_c$ is assumed to be the relationship between the outlet average velocity, u_0, and the half-height $L/2$. Hence, a Deborah number for flow-sensitive fluids is expressed as (Ryssel and Brunn[1]):

$$\mathrm{Wi}_i = \lambda_i \dot{y}_c = \frac{2\lambda_i u_0}{L} \qquad (6)$$

where subscript i is related to extensional ($i=x$) or shearing ($i=s$) viscosity functions given by Eq. (2). The Reynolds number,

$$\mathrm{Re} = \frac{\rho u_0 L}{\eta_{0_s}} \qquad (7)$$

is set equal to one in all simulated flows, and η_{∞_s} and η_{∞_x} are taken equal to zero. Three different flow-type sensitive fluids are considered: (i) for De=0.4, a shear-thinning fluid (η_s=0.1; η_x=1.0); (ii) for De=0.6, a shear-thinning and extension-thickening fluid (η_s=0.5; η_x=1.5); and (iii) for De=0.6, an extension-thickening fluid (η_s=1.0; η_x=2.5).

(a)

(b)

Figure 2. Newtonian fluid flow: (a) flow classifier R_r; (b) flow streamlines.

Figure 2a shows, for a Newtonian fluid, the distribution of the flow classifier R_r along the channel. It can be noticed that R_r=1 for most of the channel, since the Newtonian flow can be classified as a shear-dominated one. Despite that, at the entrance of the contraction, an extensional zone (R_r=0) can be noticed, due to the channel narrowness. In addition, a rigid body zone ($R_r \rightarrow 2$) can be distinguished near the contraction corner, in which a small vortex (since Re=1) is captured—see flow streamlines in Fig. 2b.

In Fig. 3, the dimensionless viscosity field, $\eta^*=\eta/\eta_0$, is presented for all studied fluids. For the shear-thinning fluid illustrated in Fig. 3a, it can be verified a viscosity decay ($\eta^* <1$) near the wall of the smaller channel, a region subjected to high shear rates. At entrance of the contraction, the viscosity does not decay, since it is a region subjected to near extensional flow, with the flow classifier R_r is around zero. In Fig. 3b, for the shear-thinning and extension-thickening fluid, a viscosity increasing ($\eta^*>1$) can be noticed at the extensional region near the contraction entrance and a viscosity reduction ($\eta^*<1$) at the shear zone near the wall of the smaller channel. In Fig. 3c, for the extension-thickening fluid, a viscosity increase ($\eta^*>1$) only occurs in the region subjected to an extensional kinematics, i.e., the one near the entrance of the contraction. In all other regions of Fig. 3c, the viscosity distribution remains constant.
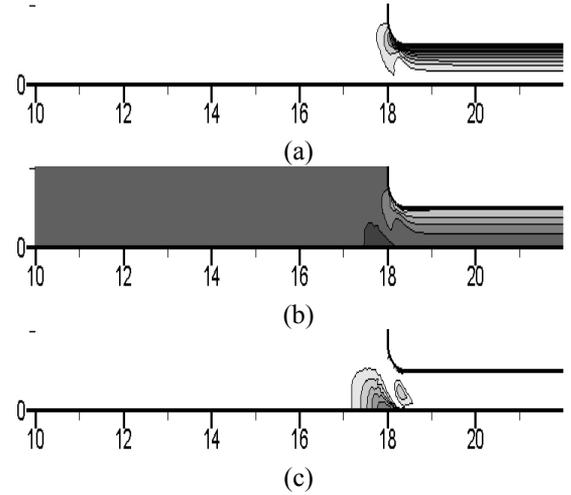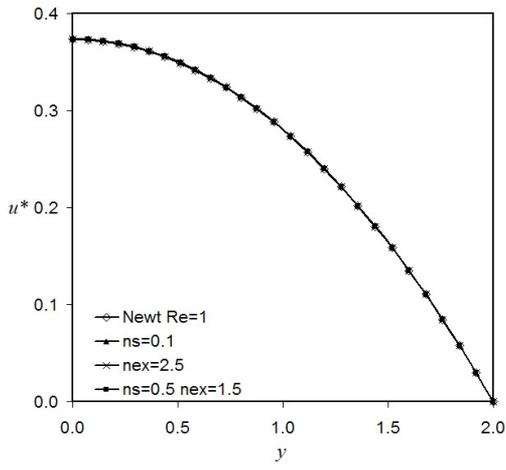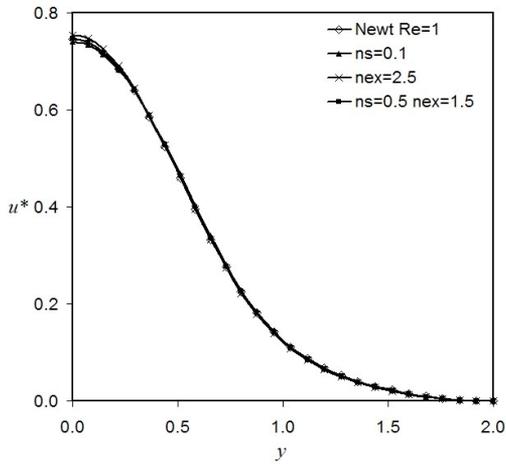

(a)

(b)

(c)

Figure 3. Viscosity function: (a) η_s=0.1 and η^*_s=1.0; (b) η^*_s=0.5 and η^*_x=1.5; (c) η^*_s=1.0 and η^*_x=2.5.

Figure 4 show transverse profiles of the dimensionless velocity $u_1^*=u_1/u_0$, at various distances from the contraction plane: (i) in Fig. 4a, at a fully-developed region upstream of the contraction, (ii) in Fig. 4b, at a region just upstream of the contraction — with Fig. 4c depicting a blown-up view
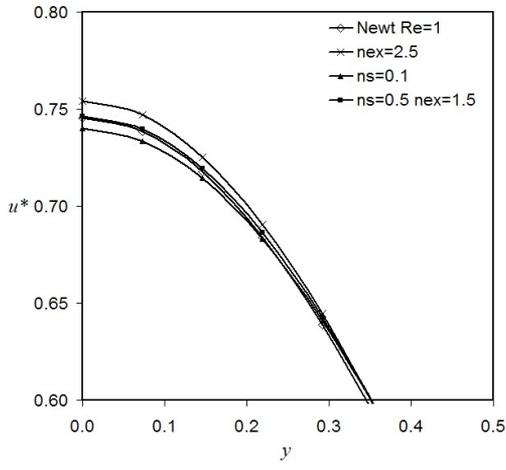
near the symmetry line; (iii) in Fig. 4d, at a region just after the entrance of the smaller channel; (iv) in Fig. 4e, at a fully-developed region downstream of the contraction.
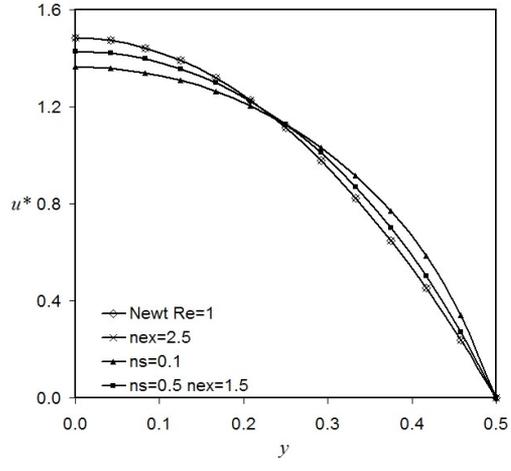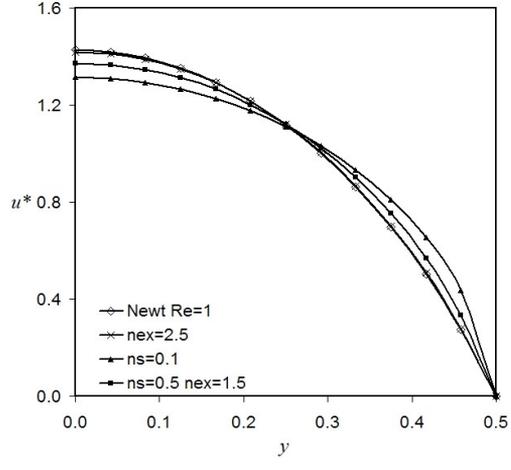

(a)

(b)

(c)

(d)

(e)

Figure 4. Velocity profiles: (a) $x_1^*=11L$; (b) $x_1^*=0.5L$; (c) $x_1^*=0.5L$ (detail); (d) $x_1^*=0.375L$, (e) $x_1^*=2.5L$.

In Fig. 4a, all fluids present similar velocity profiles at the fully-developed region upstream of the contraction, since velocity fields are not disturbed yet by elliptical effects originated from the downstream contraction. Even being this region a shear-dominated one, the strain rates are not high enough so that the shear-thinning of the viscosity can differentiate the velocity profiles. Fig. 4b seems to suggest a similar pattern for the velocity profiles. However, the blown-up view near the symmetry line (Fig. 4c) presents some distinctness: (i) the shear-thinning fluid shows a flatter profile; (ii) the shear-thinning and extension-thickening fluid,

presents a more elongated profile, with the maximum velocity slightly higher than the Newtonian one; (iii) the extensional-thickening fluid shows the highest value for the maximum velocity at the symmetry line. In the contraction region, the flow classifier R_r tends to zero at the symmetry line, characterizing an extensional region. Hence, the viscosity increasing near the symmetry line is responsible for the increasing of the maximum velocity, whereas the viscosity reduction renders flatter velocity profiles. Finally, in Fig. 4d, it is viewed that the shear-thinning fluid produces the flattest velocity profile, since just downstream of the contraction the shear rates faced in the smaller channel are high enough to cause a pronounced shear-thinning behaviour, which generates the flatten of the velocity profile —a tendency that is more evident at the fully-developed region downstream of the contraction (Fig. 4e).

Figure 5 shows dimensionless normal extra-stress profiles, $\tau_{22}{}^*=(\tau_{22}L)/(\eta_0 u_0)$, along the symmetry line. The extension-thickening fluid presents the highest value of the normal extra-stress, due to the increasing of the extensional viscosity at the entrance of the contraction. For the shear-thinning fluid), the normal extra-stress is lower than the Newtonian one, in virtue of the shearing viscosity reduction near the contraction—a decay that also affects the extra-stress distribution in the extensional region at symmetry line. At length, for the shear-thinning and extension-thickening fluid, the lower and higher values faced by the viscosity in shearing and extensional regions, respectively, prescribe an intermediate behaviour between pure extensional-thickening and pure shear-thinning ones. Moreover, $\tau_{11}{}^*$ and $\tau_{22}{}^*$ profiles are opposite to each other, as required by the flow mass conservation for a GNL model. This constrain imposed by the continuity equation leads to null normal stress differences along the channel.
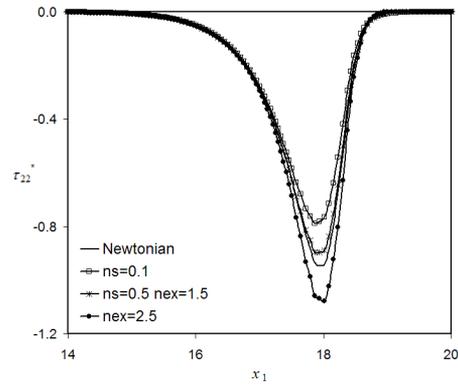

Figure 5. $\tau_{22}{}^*$ profiles along the symmetry line.

REFERENCES
1. Ryssel E, Brunn P.O. (1999a), "Flow of a quasi-Newtonian fluid through a planar contraction", *J. Non-Newtonian Fluid Mech.*, **85**, 11– 27.

2. Thompson R.L., Souza Mendes P.R. (2005), "Persistence of straining and flow classification", *Int. J. Eng. Sci.*, **43**, 79–105.

3. Behr M, Franca LP, Tezduyar TE (1993) "Stabilized finite element methods for the velocity-pressure-stress formulation of incompressible flows", *Comput. Methods Appl. Mech. Eng.*, **104**, 31–48.

4. Franca, L.P. and Frey, S. (1992), "Stabilized finite element methods: II. The incompressible Navier-Stokes equations", *Comput. Methods Appl. Mech. Eng.*, **99**, 209-233.